Published in final edited form as:
J Pharm Sci. 2013 August ; 102(8): 2450–2459. doi:10.1002/jps.23644.

Conjugation to polymeric chains of influenza drugs targeting M2 ion channels partially restores inhibition of drug-resistant mutants

Alyssa M. Larson[1], **Jianzhu Chen**[2], and **Alexander M. Klibanov**[1,3]

[1]Department of Chemistry, Massachusetts Institute of Technology, Cambridge, MA 02139

[2]David H. Koch Institute for Integrative Cancer Research and Department of Biology, Massachusetts Institute of Technology, Cambridge, MA 02139

[3]Department of Biological Engineering, Massachusetts Institute of Technology, Cambridge, MA 02139

Abstract

By attaching multiple copies of the influenza M2 ion channel inhibitors amantadine (**1**) and rimantadine (**2**) to polymeric chains we endeavored to recover their potency in inhibiting drug-resistant influenza viruses. Depending on loading densities, as well as the nature of the drug, the polymer, and the spacer arm, polymer-conjugated drugs were up to 30-fold more potent inhibitors of drug-resistant strains than their monomeric parents. In particular, a 20% loading density and a short linker group on the negatively charged poly-L-glutamate resulted in some of the most potent inhibitors for **2′**s conjugates against drug-resistant influenza strains. Although full recovery of the inhibitory action against drug-resistant strains was not achieved, this study may be a step toward salvaging anti-influenza drugs that are no longer effective.

Introduction

Influenza viruses are a commonly infect the respiratory tract in humans[1] and are a major cause of morbidity and mortality in the world.[2,3] Two of the four FDA-approved small-molecule anti-influenza drugs — the adamantane-class M2 ion-channel inhibitors amantadine (**1**) and rimantadine (**2**) (Fig. 1) — are no longer recommended as therapeutics because nearly every circulating influenza A strain has evolved resistance to them.[2,4,5] These drugs block the M2 ion channels on the surface of the virus,[6-9] thereby preventing the flow of protons into the viral core (an essential step in the viral infection cycle).[2] Resistance to **1** and **2** is due to point mutations in the M2 ion channel protein, with the most common being the S31N in the interior of the channel.[2]

Because of the daunting challenges in discovering new anti-influenza drugs, it would be of great benefit to salvage older FDA-approved drugs that are impotent against newly emerged mutants. Previously, we have demonstrated that the attachment of multiple copies of the influenza neuraminidase inhibitor zanamivir to a flexible polymeric chain not only dramatically improves the potency against drug-sensitive strains, but also resurrects the inhibitory effect against zanamivir-resistant mutants.[10,11] This phenomenon appears to stem from two mechanisms. The first is multivalency, whereby several simultaneous interactions between polymer-attached zanamivir and its viral target result in a far greater avidity compared to the monomer's binding constant,[10,12,13] while also generating an increased drug concentration in the vicinity of the virus.[13] The second contributor to the improved potency is a novel mechanism of inhibition, blocking earlier stages of the viral cycle, which monomeric zanamivir lacks.[3] Herein we explore whether the approach of attaching multiple

copies of influenza drugs to polymeric chains can boost the adamantane inhibitors' prowess against drug-resistant influenza mutants (as it did with zanamivir[10]).

Materials and Methods

Materials

Amantadine·HCl (**1**; here and henceforth the bold number equally applies to a free base/acid and its salt), rimantadine·HCl (**2**), 3-amino-1-adamantanecarboxylic acid (**3**), 3-(1-aminoethyl)adamantan-1-ol·HCl (**7**), poly-L-glutamate Na salt (MW of 50-100 kDa), carboxymethylcellulose Na salt (MW of ~100 kDa) (CMC), poly(acrylic acid) (MW of ~100 kDa), and all solvents and other reagents were purchased from Sigma Aldrich Chemical Co. (St. Louis, MO) and used without further purification unless otherwise specified. N-Hydroxysulfosuccinimide (sulfo-NHS) was from Proteochem (Denver, CO), 5-azidopentanoic acid and 5-azidopentan-1-amine from Synthonix (Wake Forest, NC), and 11-azido-3,6,9-trioxaundecanoic acid from TCI America (Portland, OR).

Syntheses

Synthesis of 1-linker-azide (6)—Linker addition to **3** was carried out as described by Wanka *et al.*[14] Briefly, 300 mg (1.5 mmol) of **3** and 715 mg (6.7 mmol) of Na_2CO_3 were suspended in a mixture of 10 mL of H_2O and 5 mL of acetone, followed by stirring and placing in an ice bath. Next, Fmoc-Cl (426 mg, 1.6 mmol) in 5 mL of acetone was added over 30 min with an addition funnel. The reaction mixture was incubated at room temperature (RT) overnight and then heated to 50°C for 2 h to evaporate acetone. To purify the product, the reaction was poured over ice (35 grams) and extracted thrice with diethyl ether. The aqueous layer was then acidified to pH 5 and extracted thrice with ethyl acetate. The ethyl acetate portions were combined, washed with H_2O, and dried over Na_2SO_4 to afford an off-white powder of Fmoc-3-amino-1-adamantanecarboxylic acid (**4**) (~40% yield). R_f on TLC silica plate of 0.47 in 10:1 (v/v) CH_2Cl_2:MeOH. ^{1}H NMR **4** ([D_8]THF) δ (400 MHz): 1.65 (2H, d, C*H*$_2$-**1**), 1.72 (2H, s, C*H*$_2$-**1**), 1.83 (4H, s, C*H*$_2$-**1**), 1.95 (4H, s, C*H*$_2$-**1**), 2.07 (H, s, C*H*-**1**), 2.14 (H, s, C*H*-**1**), 4.18 (1H, t, C*H*-Fmoc), 4.27 (2H, d, C*H*$_2$-Fmoc), 7.25 (2H, t, C*H*-aromatic-Fmoc), 7.3 (2H, t, C*H*-aromatic-Fmoc), 7.6 (2H, d, C*H*-aromatic-Fmoc), 7.8 (2H, d, C*H*-aromatic-Fmoc).

To synthesize **5, 4** (220 mg, 0.53 mmol) was dissolved in 5 mL of dry THF. To that, O-benzotriazole-*N,N,N′,N′*-tetramethyl-uronium-hexafluoro-phosphate (HBTU) (200 mg, 0.53 mmol) was added, followed by 65 μL (0.53 mmol) of 5-azidopentan-1-amine and 68 μL (0.5 mmol) of Hünig's base. The reaction mixture was stirred at RT overnight and then heated to 60°C for 1 h. After cooling, 3 mL of brine was added, and the mixture was extracted with $CHCl_3$ thrice. The organic phases were combined, washed with 1 M HCl, 5% $NaHCO_3$, H_2O, and brine, and then further purified on a silica gel column with 10:1 (v/v) CH_2Cl_2:methanol mobile phase to afford 5[14] (~55% yield). R_f on TLC silica plate of 0.82 in 10:1 (v/v) CH_2Cl_2:MeOH.^{1}H NMR **5** ($CDCl_3$) δ (400 MHz): 1.35 (2H, m, C*H*$_2$-linker), 1.47(2H, m, C*H*$_2$-linker), 1.6 (4H, m, C*H*$_2$-**1**, C*H*$_2$-linker), 1.78 (4H, s, C*H*$_2$-**1**), 1.85 (2H, d, C*H*$_2$-**1**), 1.95 (2H, d, C*H*$_2$-**1**), 2.05 (2H, s, C*H*$_2$-**1**), 2.18 (2H, s, C*H*-**1**), 3.2 (2H, dd, C*H*$_2$-linker), 3.24 (2H, t, C*H*$_2$-linker), 4.18 (1H, t, C*H*-Fmoc), 4.3 (2H, d, C*H*$_2$-Fmoc), 7.25 (2H, t, C*H*-aromatic-Fmoc), 7.3 (2H, t, C*H*-aromatic-Fmoc), 7.6 (2H, d, C*H*-aromatic-Fmoc), 7.7 (2H, d, C*H*-aromatic-Fmoc).

To generate the deprotected final **1**-linker-azide (**6**) for attachment to poly-L-glutamate, **5** (75 mg, 0.14mmol) was dissolved in 1.2 mL of dry acetonitrile and cooled to 0°C. Diethylamine (1.2 mL) was added, and the reaction mixture was stirred for 1 h at 0°C and RT for 24 h. The reaction mixture was then extracted with H_2O at pH 3, and the product (**6**)

was recovered from the aqueous phase[14] (~20% yield). R_f on TLC silica plate of 0.12 in 10:1 (v/v) CH_2Cl_2:MeOH.^{1}H NMR **6** ($CDCl_3$) δ (400 MHz): 1.27 (2H, m, C*H*$_2$-linker), 1.45(2H, m, C*H*$_2$-linker), 1.52 (2H, m, C*H*$_2$-linker), 1.61 (2H, s, C*H*$_2$-**1**), 1.7 (2H, d, C*H*$_2$-**1**), 1.78 (4H, d, C*H*$_2$-**1**), 1.83 (2H, d, C*H*$_2$-**1**), 1.88 (2H, s, C*H*$_2$-**1**), 3.1 (2H, t, C*H*$_2$-linker), 2.25 (2H, s, C*H*-**1**), 3.25 (2H, t, C*H*$_2$-linker).

Synthesis of 2-linker-azides (11 and 12)—To obtain an organic solvent soluble free base, 3-(1-aminoethyl)adamantan-1-ol·HCl was suspended in CH_2Cl_2 and washed with 1 M NaOH . The resultant organic layer was rotary-evaporated, and the isolated white powder of 3-(1-aminoethyl)adamantan-1-ol (**7**) was Boc-protected for subsequent chemical modification. To this end, a solution of di-*tert*-butyl dicarbonate (327 mg, 1.5 mmol) in 25 mL of CH_2Cl_2 was added to 5 mL of CH_2Cl_2-containing **7** (292 mg, 1.4 mmol). The reaction mixture was stirred at RT for 24 h after which it was extracted thrice with saturated Na_2CO_3 and dried over Na_2SO_4 to afford a white fluffy powder of **8**[15] (~95% yield). R_f on TLC silica plate of 0.63 in 10:1 (v/v) CH_2Cl_2:MeOH. ^{1}H NMR **8** ($CDCl_3$) δ (400 MHz): 0.98 (3H, d, C*H*$_3$-**2**), 1.33 (2H, d, C*H*$_2$-**2**), 1.39 (11H, s, *Boc*, C*H*$_2$-**2**), 1.47 (2H, s, C*H*$_2$-**2**), 1.57 (2H, d, C*H*$_2$-**2**), 1.62 (2H, d, C*H*$_2$-**2**), 1.75 (1H, s, C*H*-**2**), 2.15(2H, s, C*H*$_2$-**2**), 3.4 (1H, m, C*H*-**2**), 4.4 (1H, m, C*H*-**2**).

Next, the Boc-protected 3-(1-aminoethyl)adamantan-1-ol (**8**) was reacted with 5-azidopentanoic acid in a method similar to that of Saitoh *et al.*16 Briefly, **8** (134 mg, 0.5 mmol), 5-azidopentanoic acid (128 μL, 1.0 mmol), and 4-dimethylaminopyridine (DMAP) (6 mg, 0.03mmol) were dissolved in 3 mL of chlorobenzene. To that mixture, di(2-pyridyl)thionocarbonate (DPTC) (230 mg, 1.0 mmol) was added, and the reaction mixture was refluxed for 1 h, concentrated, and purified on a silica gel column with 2:1 (v/v) hexane:ethyl acetate mobile phase to afford **9** (~55% yield). R_f on TLC silica plate of 0.54 in 2:1 (v/v) hexane:ethyl acetate. To prepare **10**, 11-azido-3,6,9-trioxaundecanoic acid was used in place of 5-azidopentanoic acid and the reaction mixture was purified on a silica gel column with 7:1 (v/v) $CHCl_3$:acetone as a mobile phase (~65% yield). R_f on TLC silica plate of 0.60 in 7:1 (v/v) $CHCl_3$:acetone. ^{1}H NMR **9** ($CDCl_3$) δ (400 MHz): 0.98 (3H, d, C*H*$_3$-**2**), 1.35 (11H, s, *Boc*, C*H*$_2$-**2**), 1.45 (2H, d, C*H*$_2$-**2**), 1.57 (4H, m, C*H*$_2$-linker), 1.75 (2H, m, C*H*$_2$-**2**), 1.95 (3H, m, C*H*$_2$-**2**, C*H*-**2**), 2.05 (2H, d, C*H*$_2$-**2**), 2.2 (4H, m, C*H*$_2$-**2**, C*H*$_2$-linker), 3.22 (2H, m, C*H*$_2$-linker), 3.4 (1H, m, C*H*-**2**), 4.35 (1H, m, C*H*-**2**). ^{1}H NMR **10** ($CDCl_3$) δ (400 MHz): 0.95 (3H, d, C*H*$_3$-**2**), 1.35 (11H, s, Boc, C*H*$_2$-**2**), 1.43 (2H, d, C*H*$_2$-**2**), 1.54 (2H, d, C*H*$_2$-**2**), 1.78 (2H, m, C*H*$_2$-**2**), 1.93 (2H, d, C*H*$_2$-**2**), 2.03 (2H, d, C*H*$_2$-**2**), 2.09 (1H, s, C*H*-**2**), 2.17 (2H, s, C*H*$_2$-**2**), 3.3 (2H, t, C*H*$_2$-linker), 3.6 (11, m, C*H*$_2$-linker, C*H*-**2**), 3.93 (2H, s, C*H*$_2$-linker), 4.35 (1H, m, C*H*-**2**).

Deprotection of the Boc group was performed with 4 M HCl in dioxane, as described previously,[17] to yield the final **2**-linker-azide conjugates (**11** and **12**) (~90% yield). R_f on TLC silica plate of 0 in 2:1 (v/v) hexane:ethyl acetate. ^{1}H NMR **11** ($CDCl_3$) δ (400 MHz): 1.2 (3H, d, C*H*$_3$-**2**), 1.5 (8H, m, C*H*$_2$-**2**, C*H*$_2$-linker), 1.65 (1H, d, C*H*-**2**), 1.75 (4H, s, C*H*$_2$-**2**), 2.05 (2H, s, C*H*$_2$-**2**), 2.15 (2H, t, C*H*$_2$-linker), 2.2 (2H, s, C*H*$_2$-**2**), 2.95 (1H, t, C*H*-**2**), 3.2 (2H, t, C*H*$_2$-linker), 4.3 (1H, d, C*H*-**2**). ^{1}H NMR **12** ($CDCl_3$) δ (400 MHz): 1.3 (3H, d, C*H*$_3$-**2**), 1.5 (2H, d, C*H*$_2$-**2**), 1.6 (2H, s, C*H*$_2$-**2**), 1.72 (1H, d, C*H*-**2**), 1.92 (4H, m, C*H*$_2$-**2**), 2.1 (2H, d, C*H*$_2$-**2**), 2.25 (2H, s, C*H*$_2$-**2**), 3.0 (1H, s, C*H*-**2**), 3.33 (2H, t, C*H*$_2$-linker), 3.62 (11H, s, C*H*$_2$-linker, C*H*-**2**), 3.95 (2H, s, C*H*$_2$-linker).

Because of the more facile nature and higher yields of the **2**-linker-azide synthesis, we utilized **2** for our extensive structure-activity relationship of the drug-polymer conjugates.

Polymer activation—Polymers were activated with propargylamine to incorporate a terminal alkyne for subsequent conjugation reactions with the aforementioned azide-containing inhibitors **6**, **11**, and **12**. As a representative example, poly-L-glutamate Na salt (100 mg) was dissolved in 30 mL of H_2O. To that was added 300 mg of 4-(4,6-dimethoxy-1,3,5-triazin-2-yl)-4-methylmorpholinium chloride (DMTMM) (1.1 mmol) and 7 μL (0.15 mmol) of propargylamine to afford a ~10% derivatized polymer. The reaction mixture was stirred for 5 h and purified as described previously.[18,19] The amount of propargyl amine was varied to tune the % of derivatization of the polymer used. The % of derivatization was verified by ^{1}H NMR where the integration of one propargylamine H peak (the alkyne singlet hydrogen) was compared to that of the integration of one known polymer H peak (the singlet hydrogen from the poly-L-glutamate backbone).

For compounds **21** and **22**, poly-L-glutamate was reacted as described above with propargylamine and approximately 0.2 mol-eq. of either benzylamine or 2,2-dimethyl-1-propanime, respectively.

To generate a poly-L-glutamine backbone for compound **23**, the purified polymer pre-derivatized to have ~20% of its monomeric units activated with propargylamine was dissolved at 10 mg/mL in 0.1 M 2-*N*-morpholinoethanesulfonate (MES) buffer, pH 6, containing 0.5 M NaCl. To that mixture was added 1.2 mol-eq. of both 1-ethyl-3-(3-dimethylaminopropyl)carbodiimide and sulfo-NHS. The reaction mixture was stirred for 30 min at RT, after which an excess of saturated aqueous NH_4OH was added. Following an overnight incubation, the product was purified for subsequent small molecule derivatization.[18]

Polymer conjugation—Once the propargylamine-derivatized polymers were purified and quantified, they were reacted in a Cu^+-catalyzed [3+2] azide-alkyne cycloaddition with the azide containing amantadine or rimantadine derivatives (**6**, **11**, and **12**) as previously described.[18] **1′**s or **2′**s % of derivatization for each polymer-conjugate was determined by ^{1}H NMR by comparing the integrated peak for the newly formed triazole hydrogen to that for the singlet hydrogen from the poly-L-glutamate backbone. An example ^{1}H NMR breakdown is described. ^{1}H NMR **16** (D_2O) δ (600 MHz): 1.2 (3H, d, C*H*$_3$-**2**), 1.5 (8H, s, C*H*$_2$-**2**, C*H*$_2$-linker), 2.0 (2H, m, C*H*$_2$-polymer, 8H C*H*$_2$-**2**, C*H*-**2**), 2.3 (2H, s, C*H*$_2$-polymer, 4H, s, C*H*$_2$-**2**, C*H*$_2$-linker), 3.1 (1H, s, C*H*-**2**), 4.3 (1H, s, C*H*-polymer, 4H, d, C*H*$_2$-**2**, C*H*$_2$-propargylamine), 8.0 (1H, s, C*H*-triazole). Efficiency for the azide-alkyne cycloaddition ranged from approximately 70% to 100% for the small molecules. Representative ^{1}H NMR spectra are presented in the supporting information (Figures S1-S4).

Cells, viruses, and antiviral assays—Madin-Darby canine kidney (MDCK) cells for use in plaque reduction assays were from the American Type Culture Collection and maintained as described previously.[11,20] The human wild-type influenza strains A/Wuhan/359/95 (H3N2) and A/PR/8/34 (H1N1) were obtained from the U.S. Centers for Disease Control and Prevention (Atlanta, GA) and Charles River Laboratories (North Franklin, CT), respectively. The influenza strain A/WSN/33 (H1N1) was a gift from Dr. Peter Palese of Mount Sinai School of Medicine (NY, NY). Viruses were stored in a −80°C freezer and diluted in phosphate-buffered saline (PBS) for use in assays.

Plaque reduction assays with MDCK cells were carried out to determine the half-maximal inhibitory concentration (IC_{50}) of both monomeric and polymer-attached compounds as described before.[10,11,18] When analyzing polymer conjugates, the IC_{50} values were calculated based on the concentration of the small-molecule inhibitors. In investigating the effect of the inhibitors' presence for the complete viral cycle (denoted herein as “In Agar”),

equal concentrations of inhibitors were used for both pre-incubation with the virus and in the nutrient agar overlay.[18]

Results and Discussion

Syntheses

To covalently attach multiple copies of amantadine (**1**) and rimantadine (**2**) to polymeric chains without chemically modifying their amine moieties (revealed by protein X-ray crystallography to be oriented toward interior of the virion upon binding[6] and hence presumably important), we sought structural analogs of **1** and **2** with readily functionalizable groups on the opposite side of the molecules. Since commercially available 3-amino-1-adamantanecarboxylic acid (**3**) and 3-(1-aminoethyl)adamantan-1-ol (**7**) fit this description, we employed them as starting points.

Both **3** and **7** were first derivatized for polymer attachment through a series of chemical reactions depicted in Figures 2 and 3. Since our previous studies (albeit with another influenza inhibitor) demonstrated the benefits of a linker (spacer arm) between the drug and the polymeric backbone in reducing steric hindrances,[18] we also decided to insert a linker between **3** or **7** and the polymers used. As seen in Figs. 2 and 3, first the drugs' amino groups were protected by Fmoc and Boc groups, respectively, followed by linker attachment and amine deprotection to afford **1** and **2** with azide terminating linkers to be subsequently used for conjugation to polymers. Our initial studies herein utilized poly-L-glutamate as a polymer because it is benign, freely water-soluble, biodegradable, and non-immunogenic.[10]

Amantadine (1) and its polymer conjugates

To verify which strains were resistant to the adamantane class of inhibitors, we determined the IC_{50} values for monomeric **1** against three representative influenza strains using the plaque reduction assay. They were A/Wuhan/359/95 (herein denoted as “Wuhan”), a human strain ***with no known resistance*** to the adamantane class of influenza inhibitors; A/PR/8/34 (herein denoted as “PR8”), a human strain ***with documented resistance*** to the adamantanes;[21] and A/WSN/33 (herein denoted as “WSN”), a laboratory-adapted human strain also ***with known resistance*** to the adamantanes.[21] As seen in the 1st line of Table 1 (the first three data columns), the non-resistant Wuhan strain was indeed quite sensitive to **1** with an IC_{50} of 60 ± 24 μM. In contrast, the drug-resistant PR8 and WSN strains were both far less sensitive toward the inhibitor with much poorer IC_{50} values of 2.2 ± 0.66 mM and 3.4 ± 0.2 mM, respectively, thus illustrating why **1** is no longer recommended for therapeutic use.

When **6** was attached to poly-L-glutamate at a ~7% loading (i.e., ~7% of all the monomeric units on the polymeric chain were drug-decorated), the inhibition for the resultant compound **13** (Figure 4) was nearly the same for the Wuhan and PR8 strains; for WSN, however, **13** was some 4-fold better inhibitor than **1** (Table 1, the first three data columns). When the degree of loading was roughly doubled (to yield compound **14** in Fig. 4), the inhibition for both the PR8 and WSN strains improved a few fold. Note that the original **1′**s precursor **3** could not be tested as a monomer in the plaque reduction assay to determine the effect of adding a –COOH to the structure because of its poor solubility in aqueous PBS, which is the medium used in our antiviral assays.

We then investigated whether a further improvement in anti-influenza potency of the polymer conjugates **13** and **14** over the monomeric **1** could be attained by lengthening the time of their contact with the viruses during the assay. In our standard plaque reduction assay (designated as “Not in Agar” in Table 1), compounds are incubated with the viruses

for 1 h prior to infection and during the subsequent 1-h infection period. After that, the inhibitors are removed, and fresh nutrient agar replaces them for the duration of the assay (while plaque formation occurs). Therefore, in the next series of experiments, we decided to keep the inhibitors present not only during those initial steps of the assay but also in an equal concentration in the nutrient agar overlay to allow them to act on all subsequent steps in the viral cycle.

As seen in Table 1 (the "In Agar" data columns), including the inhibitor for the entire plaque reduction assay improved IC_{50} values in most instances. With **13** and **14**, we observed no improvement in IC_{50} values over **1** for the Wuhan strain but several-fold improvements for the PR8 and WSN strains. Thus although the inclusion in the agar results in ***net*** lower IC_{50} values for most of the compounds tested, a greater ***magnitude*** of the improvement over the monomer (**1**) was seen when polymer conjugates were present only at initial steps of viral infection. Overall, however, these data show a marginal recovery in inhibitory potency toward drug-resistant strains when multiple copies of **1** are attached to poly-L-glutamate.

Rimantadine (2) and its polymer conjugates

We next explored how the other FDA-approved M2 ion channel inhibitor, **2**, as well as its multiple copies attached to poly-L-glutamate, behaved against the aforementioned influenza strains. As in the case of **1**, the Wuhan strain was very sensitive to **2** with an even better IC_{50} value of 2.7 ± 1.4 μM, while both the PR8 and WSN strains were far less sensitive with IC_{50}s well into the low-single-millimolar range (Table 2), again confirming the reported drug resistance patterns.[21] We then tested the effect of the insertion of an OH group into **2′**s scaffold (to yield **7**, which was used in subsequent derivatization (Fig. 3)). This small group greatly diminished the inhibitory potency against the Wuhan strain raising the IC_{50} some ~90-fold (Table 2, first data column, 2nd line). The addition of an OH group also deleteriously, albeit less drastically, affected the already sub-optimal inhibition for the resistant strains (Table 2, second and third data columns, 2nd line). Previous studies have also demonstrated that the addition of a linker group to a small-molecule inhibitor can negatively affect its inhibitory potency.[10,18] (This decline can be overcome, however, though multivalency.) That even a small addition, such as an OH group, has this deleterious effect demonstrates how subtle the structure-activity relationship is in this case.

Covalent attachment of **11** to poly-L-glutamate at a ~10% loading (compound **15**, Fig. 4) afforded a significant improvement for all three viral strains over **7** (Table 2, the first three data columns, 3rd line). When compared to the native inhibitor (**2**), however, the polymer conjugation did not fully overcome the negative effects of the OH for the Wuhan strain leaving the IC_{50} value at 24 ± 5 μM, i.e., some 10-fold inferior to **2′**s. The attachment to poly-L-glutamate at a ~10% loading did little for the inhibitory effect against the PR8 strain but improved the IC_{50} for WSN some 4-fold over **2**.

Effect of the degree of loading on rimantadine-polymer conjugates

Since our initial studies with **1** yielded an improvement when the loading of the inhibitor on the polymeric chain was increased (Table 1), we explored whether **2** also followed this trend. As seen in Table 2 (4^{th} line, the first three data columns), increasing the loading to ~20% (compound **16**, Fig. 4) afforded some of the most potent poly-L-glutamate conjugates: although the IC_{50} for **16** was still 10-fold worse than **2′**s for the Wuhan strain, for PR8 and WSN we saw 8-fold and 30-fold improvements over **2**, respectively. Interestingly, further increasing the degree of loading to ~30% and then to ~43% (compounds **17** and **18**, respectively, Fig. 4) gave little additional improvement or even yielded worse inhibitors (Table 2).

When testing the polymeric inhibitors **15**, **16**, **17**, and **18** for the duration of the plaque reduction assay (Table 2, the "In Agar" columns), patterns similar to those in the experiments with **1** were observed: the net IC_{50} was improved in most cases, but the magnitude of improvement over the monomer (**2**) became smaller. The optimal degree of loading also became less clear for the PR8 strain because all compounds had nearly the same IC_{50} values.

Effect of linker's properties on rimantadine-polymer conjugates

We next determined whether a slightly longer and more hydrophilic spacer arm between **2** and poly-L-glutamate would be of benefit. Figure 3 depicts the synthetic route to compound **12** which contains a hydrophilic, poly(ethylene glycol), linker and six extra atoms between the drug and the polymeric chain. As seen in Table 2, when **12** is attached to poly-L-glutamate at a ~10% loading to generate compound **19** (Fig. 4), there was little or no improvement in inhibition over **2** (some 70-fold worse for the Wuhan strain, no change for PR8, and approximately a 3-fold improvement for WSN). When the loading was increased to ~20% (compound **20**), which was optimal for the shorter and more hydrophobic linker, the inhibition was improved compared to **19**: only a 18-fold worse inhibition for the Wuhan strain and a 13-fold improvements for both PR8 and WSN over **2** (Table 2).

When assaying **19** and **20** for the duration of the assay (Table 2, "In Agar"), no sizable benefit to the longer incubation was observed again and, in fact, **19** exhibited toxic effects in this modality. Since the slightly longer and more hydrophilic linker failed to generate ***major*** improvements compared to the shorter and more hydrophobic one, we decided to continue our studies with the latter.

Effect of polymer's structure on rimantadine-polymer conjugates

To determine whether increasing hydrophobicity of the polymeric backbone by inserting extra aromatic or aliphatic hydrophobic moieties into it would improve inhibition, perhaps due to extra interactions between the polymer and the viral surface,[12] we synthesized **21** containing ~20% of benzyl rings in addition to a ~15% loading of **2**, as well as **22** containing ~25% of *tert*-butyl substituents in addition to ~20% of **2** moieties (Fig. 5). When conjugate **21** was tested against all three influenza strains in the plaque reduction assay, we observed similar improvements over **2** compared to that afforded by poly-L-glutamate with ~20% loading and no additional hydrophobic moieties (**16**) for the Wuhan and PR8 strains, and not as marked improvements for the WSN strain: some 18-fold weaker inhibition than the monomer for the Wuhan strain and 16/17-fold improvements for WSN and PR8 (Table 2). Similarly, for the *tert*-butyl-derivatized poly-L-glutamate conjugate **22**, we saw the same 18-fold decline in improvement over **2** for the Wuhan strain and some 10- and 22-fold improvements over **2** for PR8 and WSN, respectively. Therefore, although the addition of hydrophobic groups to the polymer in some cases did lead to a modest improvement over the 20%-derivatized plain poly-L-glutamate, there was no compelling reason for their inclusion.

We also examined the role of polymer's characteristics in the conjugate's inhibitory potency. To this end, first the charge of the poly-L-glutamate backbone was abolished by transforming it into the neutral poly-L-glutamine (compound **23**, Fig. 6). As seen in Table 2, the neutralization of the polymer resulted in no improvements and actually in over 20-fold weaker inhibition than with the monomeric **2** for the Wuhan strain. For PR8 and WSN, **23** afforded 2- and 12-fold improvements, respectively, over **2**, which is worse than **23′**s negatively charged counterpart, **16**. When incubated with the viruses for the duration of the assay, **23** exhibited improvements over the monomer for the PR8 and WSN strains, but not marked ones (Table 2, "In Agar"). Thus, putative electrostatic repulsions between the virus

and polymer are not a significant factor in viral inhibition for our system (in contrast to observations in previous studies[10,12]); also, the neutralization of the poly-L-glutamate backbone to form poly-L-glutamine generated less potent inhibitors for drug-polymer conjugates at the same degree of small-molecule loading.

To investigate how new, structurally unrelated polymeric backbones would affect the inhibition of drug-resistant influenza viruses by polymer-conjugated **2**, the dissimilar polymers poly(acrylic acid Na salt) and carboxymethylcellulose Na salt (CMC) were employed. Since each of these polymers, like poly-L-glutamate, contained carboxylate moieties, the same conjugation chemistry could be carried out.

Polyacrylate with ~10% of its monomeric units derivatized with **2** (compound **24**, Fig. 6) was superior to all other conjugates tested against the Wuhan strain: it overcame ***all*** negative effects from an OH addition to **2** with an IC_{50} equal to that of the commercial drug itself (Table 2). However, against the other two influenza strains **24** did not possess the same potency with IC_{50} values of 120 ± 50 and 280 ± 50 μM for PR8 and WSN, thus resulting in some 11- and 8-fold improvements, respectively, over **2** for these drug-resistant strains (Table 2). Compound **24** was, however, markedly better than other 10%-modified polymer-conjugates (**15** and **19**), suggesting that the polyacrylate backbone is a promising lead for multivalent inhibitors.[12,13]

Attachment of **2** to CMC at a ~20% loading (**25**, Fig. 6) drastically curtailed inhibition of the Wuhan strain, with an IC_{50} of 760 ± 160 μM (Table 2). Similarly poor IC_{50} values were obtained against PR8 and WSN (1,200 ± 800 and 780 ± 90 μM, respectively) suggesting that the inhibition afforded by these compounds might not even be caused by **2′**s action *per se* but be due to CMC's intrinsic weak antiviral activity.

In closing, in this study we have attached multiple copies of influenza M2 ion-channel inhibitors to a variety of polymers in an attempt to ameliorate, if not salvage, their ability to inhibit adamantane-resistant influenza strains. Our previous studies have shown that for another influenza virus inhibitor, zanamivir, polymer conjugation to form multivalent inhibitors could completely overcome resistance in zanamivir-resistant strains.[10] However, zanamivir binds to its target neuraminidase on the outermost solvent-exposed portion of the enzyme[2,22] which is presumably readily accessed to the drug-polymer conjugate. In contrast, the M2 ion channel imbedded within the viral membrane could be more difficult to access, thereby hindering multivalency. Additionally, the neuraminidase's greater abundance on the viral surface (about 100 copies per virion compared to some 20 copies for the M2 ion channel)[22] may also play a role in our incomplete potency recovery. Nonetheless, a progress toward our goal of recovering the adamantane inhibitors has been made by preparing **2**-polymer conjugates up to 30-fold more potent than their monomeric precursors against some drug-resistant influenza strains.

Supplementary Material

Refer to Web version on PubMed Central for supplementary material.

Acknowledgments

This work was partially supported by the National Institutes of Health grant U01-AI074443. AML was a recipient of a Martin Family graduate fellowship.

References

1. Taubenberger JK, Morens DM. The pathology of influenza virus infections. Ann Rev Pathol. 2008; 3:499–522. [PubMed: 18039138]
2. De Clercq E. Antiviral agents active against influenza A viruses. Nature Revs Drug Discov. 2006; 5:1015–1025. [PubMed: 17139286]
3. Lee CM, Weight AK, Haldar J, Wang L, Klibanov AM, Chen J. Polymer-attached zanamivir inhibits synergistically both early and late stages of influenza virus infection. Proc Natl Acad Sci USA. 2012; 109:20385–20390. [PubMed: 23185023]
4. Bright RA, Shay DK, Shu B, Cox NJ, Klimov AI. Adamantane resistance among influenza A viruses isolated early during the 2005-2006 influenza season in the United States. JAMA. 2006; 295:891–894. [PubMed: 16456087]
5. Das K, Aramini JM, Ma L-C, Krug RM, Arnold E. Structures of influenza A proteins and insights into antiviral drug targets. Nature Struct Molec Biol. 2010; 17:530–538. [PubMed: 20383144]
6. Stouffer AL, Acharya R, Salom D, Levine AS, Di Costanzo L, Soto CS, Tereshko V, Nanda V, Stayrook S, DeGrado WF. Structural basis for the function and inhibition of an influenza virus proton channel. Nature. 2008; 451:596–599. [PubMed: 18235504]
7. Kozakov D, Chuang G-Y, Beglov D, Vajda S. Where does amantadine bind to the influenza virus M2 proton channel? Trends Biochem Sci. 2010; 35:471–475. [PubMed: 20382026]
8. Pielak RM, Schnell JR, Chou JJ. Mechanism of drug inhibition and drug resistance of influenza A M2 channel. Proc Natl Acad Sci USA. 2009; 106:7379–7384. [PubMed: 19383794]
9. Cady SD, Schmidt-Rohr K, Wang J, Soto CS, DeGrado WF, Hong M. Structure of the amantadine binding site of influenza M2 proton channels in lipid bilayers. Nature. 2010; 463:689–692. [PubMed: 20130653]
10. Weight AK, Haldar J, de Cienfuegos LA, Gubareva LV, Tumpey TM, Chen J, Klibanov AM. Attaching zanamivir to a polymer markedly enhances its activity against drug-resistant strains of influenza a virus. J Pharm Sci. 2011; 100:831–835. [PubMed: 20740680]
11. Haldar J, de Cienfuegos LA, Tumpey TM, Gubareva LV, Chen J, Klibanov AM. Bifunctional polymeric inhibitors of human influenza A viruses. Pharm Res. 2010; 27:259–263. [PubMed: 20013036]
12. Mammen M, Dahmann G, Whitesides GM. Effective inhibitors of hemagglutination by influenza-virus synthesized from polymers having active ester groups—Insight into mechanism of inhibition. J Med Chem. 1995; 38:4179–4190. [PubMed: 7473545]
13. Mammen M, Choi S-K, Whitesides GM. Polyvalent interactions in biological systems: implications for design and use of multivalent ligands and inhibitors. Angew Chem Int Ed. 1998; 37:2754–2794.
14. Wanka L, Cabrele C, Vanejews M, Schreiner PR. γ-Aminoadamantanecarboxylic acids through direct C–H bond amidations. Eur J Org Chem. 2007; 9:1474–1490.
15. Yi L, Abootorabi M, Wu Y-W. Semisynthesis of prenylated Rab GTPases by click ligation. ChemBioChem. 2011; 12:2413–2417. [PubMed: 21960422]
16. Saitoh K, Shiina I, Mukaiyama T. O,O′-Di-(2-pyridyl)thiocarbonate as an efficient reagent for the preparation of carboxylic esters from highly hindered alcohols. Chem Lett. 1998; 27:679–680.
17. Iossifidou S, Froussio CC. Facile synthesis of 1-adamantyl esters of L-α-amino acids, a new class of carboxy protected derivatives. Synthesis. 1996; 11:1355–1358.
18. Larson AM, Wang H, Cao Y, Jiang T, Chen J, Klibanov AM. Conjugating drug candidates to polymeric chains does not necessarily enhance anti-influenza activity. J Pharm Sci. 2012; 101:3896–3905. [PubMed: 22786697]
19. Ochs CJ, Such GK, Staedler B, Caruso F. Low-fouling, biofunctionalized, and biodegradable click capsules. Biomacromolecules. 2008; 9:3389–3396. [PubMed: 18991459]
20. Haldar J, Weight AK, Klibanov AM. Preparation, application and testing of permanent antibacterial and antiviral coatings. Nature Protocols. 2007; 2:2412–2417.
21. Bright RA, Medina MJ, Xu X, Perez-Oronoz G, Wallis TR, Davis XM, Povinelli L, Cox NJ, Klimov AI. Incidence of adamantane resistance among influenza A (H3N2) viruses isolated

worldwide from 1994 to 2005: a cause for concern. Lancet. 2005; 366:1175–1181. [PubMed: 16198766]

22. Lamb, RA.; Krug, RM. Orthomyoxoviridae: the viruses and their replication. In: Knipe, DM.; Howley, PM., editors. Fields' Virology. 5th. Philadelphia: Wolters Kluwer Health Lippincott Williams & Wilkins; 2007.

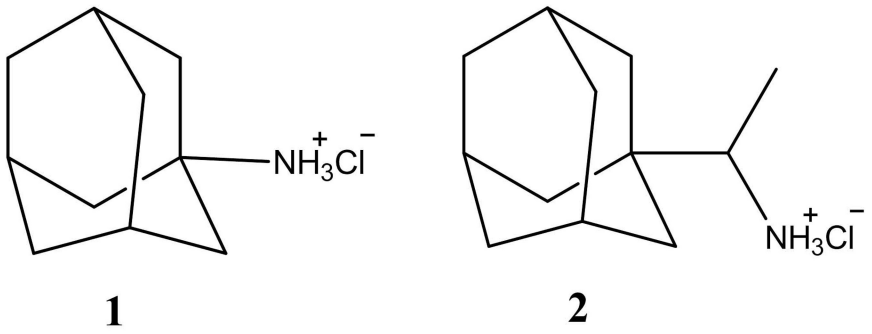

1 **2**

Figure 1.
Chemical structures of both FDA-approved adamantane-class M2 ion channel influenza A inhibitors still in therapeutic use: amantadine·HCl (**1**) and rimantadine·HCl (**2**).

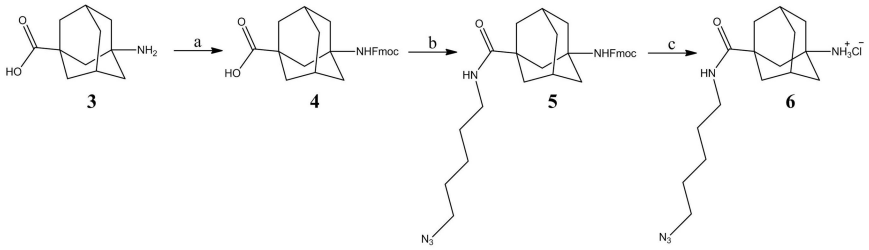

Figure 2.

Synthetic route to generating the **1**-linker-azide compound **6** for subsequent covalent attachment to poly-L-glutamate. Reagents employed: (a) Fmoc-Cl, Na_2CO_3, H_2O/acetone; (b) HBTU, 5-azidopentan-1-amine, Hünig's base, THF; and (c) anhydrous acetonitrile/ diethylamine. See Methods for details.

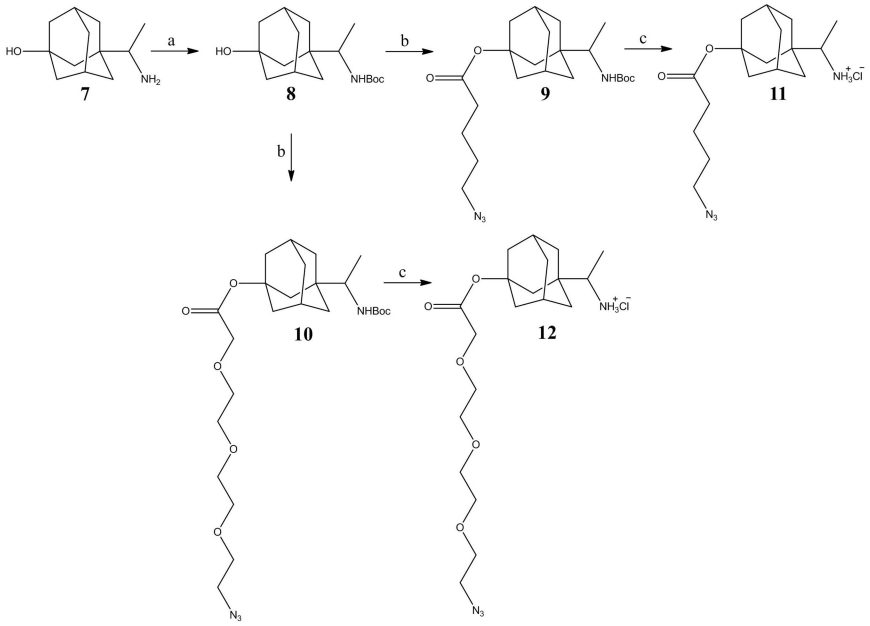

Figure 3.

Synthetic route to generating the **2**-linker-azide compounds **11** and **12** for subsequent covalent attachment to poly-L-glutamate and other polymers. Reagents employed: (a) di-*tert*-butyl dicarbonate, dichloromethane; (b) 5-azido-pentanoic acid or 11-azido-3,6,9-trioxaundecanoic acid, DPTC, DMAP, chlorobenzene (reflux); (c) 4 M HCl in dioxane. See Methods for details.

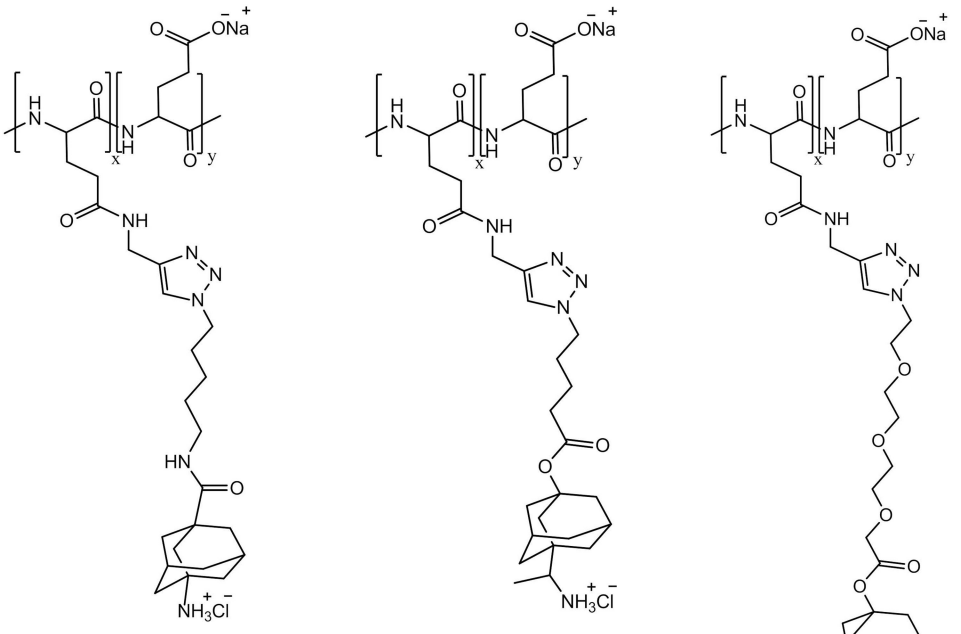

13 x:y = 7:93
14: x:y = 13:87

15: x:y = 10:90
16: x:y = 20:80
17: x:y = 30:70
18: x:y = 43:57

19: x:y = 10:90
20: x:y = 20:80

Figure 4.
Chemical structures of poly-L-glutamate-attached conjugates of **1** and **2** at various degrees of loading (% of derivatization).

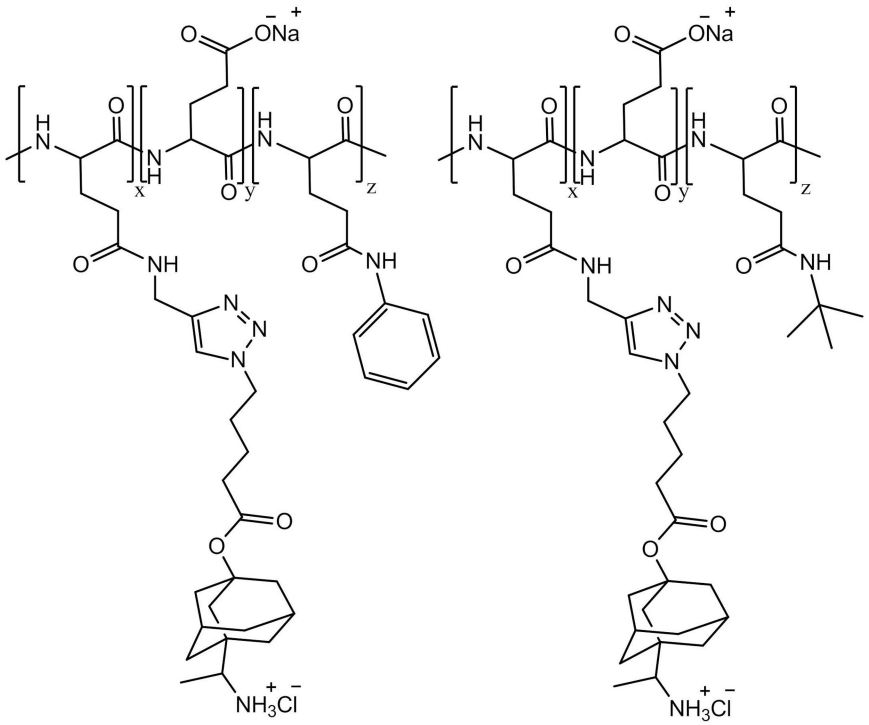

21: x:y:z = 15:20:65 **22**: x:y:z = 20:25:55

Figure 5.
Chemical structures of poly-L-glutamate derivatized with ~15% of **2** of plus ~20% of benzylamine (**21**) and with ~20% of **2** plus ~25% of 2,2-dimethyl-1-propamine (**22**).

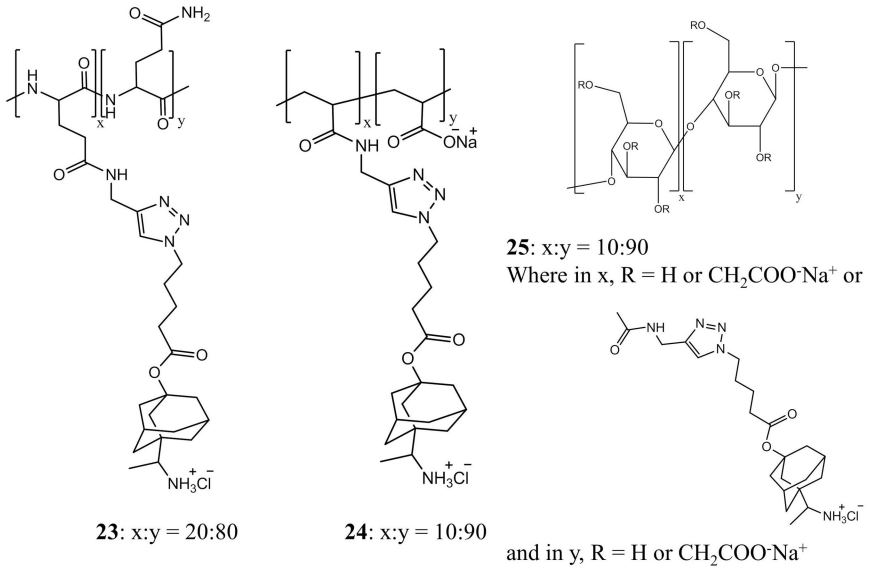

Figure 6.
Chemical structures of poly-L glutamine, poly(acrylic acid Na salt), and CMC derivatized with **2**.

Table 1

The IC_{50} values for both monomeric **1** and its poly-L-glutamate conjugates against the Wuhan, PR8, and WSN strains of influenza A virus.

	IC_{50} (μM)[a]					
	"Not in Agar"[b]			"In Agar"[c]		
Inhibitor	**Wuhan**	**PR8**	**WSN**	**Wuhan**	**PR8**	**WSN**
1	$(6.0 \pm 2.4) \times 10^1$	$(2.2 \pm 0.6) \times 10^3$	$(3.4 \pm 0.2) \times 10^3$	$(3.8 \pm 0.7) \times 10^1$	$>5 \times 10^2$	$(1.8 \pm 0.1) \times 10^2$
13	$(8.5 \pm 4.7) \times 10^1$	$(1.4 \pm 0.2) \times 10^3$	$(7.8 \pm 3.5) \times 10^2$	$(3.3 \pm 0.7) \times 10^1$	$(1.2 \pm 0.1) \times 10^2$	$(8.3 \pm 0.3) \times 10^1$
14	$(4.4 \pm 0.1) \times 10^1$	$(8.9 \pm 1.7) \times 10^2$	$(8.6 \pm 1.8) \times 10^2$	$(4.9 \pm 1.4) \times 10^1$	$(2.2 \pm 0.3) \times 10^2$	$(7.7 \pm 1.9) \times 10^1$

[a] The plaque reduction assay experiments were run in triplicate; the calculated mean and standard deviation values are presented in the table. All IC_{50} values are expressed based on the concentration of **1**. Our previous studies have demonstrated that the IC_{50} value of bare poly-L-glutamate far exceeds 1 mM.[18] Therefore, no inhibition can be attributed to the polymer itself.

[b] "Not in Agar" refers to an inhibitor present only in initial steps of infection, i.e., during a 1-h pre-incubation and subsequent viral binding to MDCK cells.

[c] "In Agar" refers to an inhibitor present during all stages of viral infection, i.e., during a 1-h pre-incubation, subsequent viral binding to MDCK cells, and the rest of the 72-h plaque reduction assay.

Table 2

The IC_{50} values for monomeric **2** and **7**, as well as for the latter's various polymer conjugates against the Wuhan, PR8, and WSN strains of influenza A virus.

	IC_{50} (μM)[a]					
	"Not in Agar"[b]			"In Agar"[c]		
Inhibitor	**Wuhan**	**PR8**	**WSN**	**Wuhan**	**PR8**	**WSN**
2	2.7 ± 1.4	(1.3 ± 0.09) × 10^3	(2.4 ± 1.2) × 10^3	1.4 ± 0.5	(3.0 ± 0.6) × 10^2	(1.9 ± 0.8) × 10^2
7	(2.4 ± 0.5) × 10^2	(3.5 ± 0.8) × 10^3	>4.3 × 10^3	(1.2 ±0.8) × 10^2	(8.6 ± 1.1) × 10^2	(5.0 ± 0.9) × 10^2
15	(2.8 ± 0.4) × 10^1	(1.5 ± 0.4) × 10^3	(6.4 ± 1.0) × 10^2	(8.0 ± 3.5) × 10^1	(1.1 ± 0.4) × 10^2	(4.2 ± 0.3) × 10^1
16	(2.5 ± 0.5) × 10^1	(1.5 ± 0.8) × 10^2	(7.7 ± 0.7) × 10^1	(4.8 ± 3.2) × 10^1	(1.4 ± 0.4) × 10^2	(5.0 ± 1.3) × 10^1
17	(1.4 ± 0.1) × 10^2	(9.3 ± 2.4) × 10^2	(3.9 ± 0.6) × 10^2	(1.5 ± 0.09) × 10^2	(1.7 ± 0.1) × 10^2	(1.8 ± 0.09) × 10^2
18	(8.0 ± 1.7) × 10^2	>1.4 × 10^3	>1.4 × 10^3	(1.5 ± 0.3) × 10^2	(1.2 ± 0.5) × 10^2	(1.8 ± 0.4) × 10^2
19	(1.9 ± 0.7) × 10^2	(1.1 ± 0.4) × 10^3	(9.2 ± 4.1) × 10^2	Tox >125[d]	Tox >125[d]	Tox>125[d]
20	(4.9 ± 0.5) × 10^1	(1.0 ± 0.5) × 10^2	(1.8 ± 1.1) × 10^2	(7.3 ± 1.8) × 10^1	(1.1 ± 0.9) × 10^2	(8.8 ± 1.3) × 10^1
21	(4.7 ± 0.8) × 10^1	(7.6 ± 2.9) × 10^1	(1.5 ± 0.5) × 10^2	n.d.	n.d.	n.d.
22	(4.9 ± 0.2) × 10^1	(1.3 ± 0.5) × 10^2	(1.1 ± 0.5) × 10^2	n.d.	n.d.	n.d.
23	(6.4 ± 1.6) × 10^1	(6.0 ± 3.6) × 10^2	(2.0 ± 0.7) × 10^2	(1.2 ± 0.3) × 10^2	(9.9 ± 0.5) × 10^1	(5.0 ± 1.6) × 10^1
24	2.5 ± 0.4	(1.2 ± 0.5) × 10^2	(2.8 ± 0.5) × 10^2	n.d.	n.d.	n.d.
25	(7.6 ± 1.6) × 10^2	(1.2 ± 0.8) × 10^3	(7.8 ± 0.9) × 10^2	n.d.	n.d.	n.d.

[a] The plaque reduction assay experiments were run in triplicate; the calculated mean and standard deviation values are presented in the table. All IC_{50} values are expressed based on the concentration of **2**; n.d. stands for "not determined". Our previous studies have demonstrated that neither poly-L-glutamate nor poly-L-glutamine possesses any intrinsic anti-influenza properties with IC_{50} values far exceeding 1 mM.[10,18] Therefore, no inhibition can be attributed to the polymers themselves.

[b] "Not in Agar" refers to an inhibitor present only in initial steps of infection, *i.e.*, during a 1-h pre-incubation and subsequent viral binding to MDCK cells.

[c] "In Agar" refers to inhibitor present during all stages of viral infection, *i.e.*, during a 1-h pre-incubation, subsequent viral binding to MDCK cells, and the rest of the 72-h plaque reduction assay.

[d] The IC_{50} value could not be determined because concentrations under 125 μM were below the IC_{50} and concentrations above were toxic to the MDCK cells (i.e., no plaques could be visualized).